Published in final edited form as:
J Neurosci Res. 2013 December ; 91(12): 1618–1627. doi:10.1002/jnr.23283.

Neural and Physiological Responses to a Cold Pressor Challenge in Healthy Adolescents

Heidi L. Richardson[1], **Paul M. Macey**[2,3], **Rajesh Kumar**[1], **Edwin M. Valladares**[1], **Mary A. Woo**[3], and **Ronald M. Harper**[1,2]

[1]Department of Neurobiology, David Geffen School of Medicine at UCLA

[2]Brain Research Institute, University of California at Los Angeles, Los Angeles, CA 90095-1763, USA

[3]School of Nursing, University of California at Los Angeles, Los Angeles, CA 90095-1763, USA

Abstract

Abnormal autonomic function is common in pediatric diseases. Assessment of central mechanisms underlying autonomic challenges may reveal vulnerabilities antecedent to system failure. Our objective was to characterize central markers and physiological responses to a cold pressor challenge in normal children as a critical step for establishing such screening. We performed functional magnetic resonance imaging (fMRI), and collected physiological measures during cold application to the foot in 24 healthy adolescents (15.5±0.4 years; 13 male). The protocol included a 120s baseline, 120s right-foot cold water immersion (4°C), and 120s recovery. Analyses included heart rate (HR) cross-correlations with fMRI signals. Cold application increased HR 13% 5-7s after onset, which remained elevated throughout the challenge. Respiratory rate transiently increased (peak 22%), then declined (nadir 12% below baseline), before normalizing at 75s. Cold onset rapidly increased somatosensory cortex and medullary signals, which fell after 25s. Right anterior insular cortex signals increased early, followed after 20s by the left anterior insula, with HR declining 8s later. Amygdalae signals also rose, but signals declined in the posterior cingulate cortex, caudate nucleus, hippocampus, and hypothalamus. Declining signals appeared late in the cerebellar fastigial nuclei (60-120s), and in the pons and thalamus. Somatosensory cortex, fastigial nuclei, and hypothalamic responses were principally left-sided, with bilateral responses elsewhere. Late left anterior insula responses likely underlie the HR decline; the late cerebellar pattern may modulate recovery. The laterality, timing and amplitude of normative responses, and rostral response differentiation indicate the complex integration of adolescent autonomic processing, and provide indices for pathological comparisons.

Keywords

Blood pressure; Magnetic resonance imaging; Heart rate; Respiratory rate; Autonomic

[*]**Corresponding Author:** Ronald M. Harper, Ph.D. Department of Neurobiology David Geffen School of Medicine at UCLA University of California at Los Angeles Los Angeles, CA 90095-1763, USA rharper@ucla.edu Tel: 310-825-5303 Fax: 310-825-2224.

CONFLICTS OF INTEREST: All authors have no conflicts of interest to declare.

INTRODUCTION

Autonomic nervous system deficits appear in multiple adolescent disease conditions. The ability to cope with pathological disturbances, especially of cardiovascular regulation, involves participation of brain autonomic regulatory areas. In affected patients, such brain areas often show distorted responses at onset or recovery of the disturbance, as well as during the perturbation. Evaluation of the nature of the distorted responses, particularly in the ability of specific brain areas to respond in a timely fashion, can help reveal underlying mechanisms contributing to the autonomic pathology. However, that determination requires measures of normal function against which responses in disease conditions can be compared. Such normative evaluations are lacking in adolescents, especially with the time course of central recruitment to major autonomic challenges.

An easily-administered non-invasive autonomic challenge is cold application to tissue, typically, cold water, which increases centrally-mediated sympathetic discharge by activating dermal thermoreceptors. The enhanced sympathetic outflow elicits peripheral vasoconstriction while increasing cardiac output and pulse pressure (Lovallo 1975; Peckerman et al. 1994). The cold pressor challenge has been employed to unveil autonomic characteristics in healthy and diseased adults, eliciting increased blood pressure and heart rate (Harper et al. 2003), and revealing central nervous system roles in blood pressure regulation.

Functional magnetic resonance imaging (fMRI) procedures provide a non-invasive means to examine central responses to autonomic challenges in both adults and adolescents (Harper et al. 2003; Kim et al. 2002; Macey et al. 2005). Both cold application to the forehead and the foot have been used for such challenges. Forehead cold application invokes the “dive reflex” which elicits substantially different autonomic outcomes with concurrent trigeminal stimulation, and recruits different neural structures from those found following cold application to the foot (Durel et al. 1993).

The objective of this study was to determine physiological and temporal patterns of central neural responses to a peripherally-mediated cold pressor challenge in healthy adolescents. This objective would establish normative levels against which distorted autonomic patterns and their control could be evaluated in pathological developmental conditions.

MATERIALS AND METHODS

Subjects

Twenty-four healthy adolescent subjects (13 male/11 female; median age 15 years, range 11-18 years) were recruited via local advertisements. Medical histories were screened extensively for indications of autonomic dysfunction, e.g. hypertension, or smoking, neurological deficits, or other medical conditions that might influence neural responses (all of which were exclusion criteria). Protocols were approved by the Institutional Review Board of the University of California at Los Angeles, and written parental/guardian consent and subject assent was obtained.

Study Protocols

Physiology Recordings—Respiratory movements, heart rate and oxygen saturation were monitored using MRI-compatible instrumentation. Respiratory effort was measured using a thoracic pressure-sensing air-filled bag. Pulse finger oximetry assessed the raw plethysmographic waveform and oxygen saturation (Nonin 8600FO, Plymouth MN, USA). Physiologic signals were recorded on a laptop acquisition system (InstruNet; GW Instruments, Somerville MA, USA), with breathing sampled at 100Hz and pulse oximeter signals at 1KHz.

Magnetic Resonance Imaging—Subjects lay supine in a 3.0 Tesla MRI scanner (Siemens Magnetom Tim-Trio, Erlangen, Germany); foam pads on either side of the head minimized head motion. For anatomical evaluation, high resolution T1-weighted images were collected using a magnetization prepared rapid acquisition gradient echo pulse sequence [repetition time (TR) = 2200ms; echo time (TE) = 3.05ms; inversion-time = 1100ms; flip-angle = 10°; matrix size = 256×256; field of view (FOV) = 220×220mm; slice thickness = 1.0mm; slices = 176]. Proton-density (PD) and T2-weighted images were also collected, using a dual-echo turbo spin-echo pulse sequence (TR = 8000ms; TE1, 2 = 17, 133ms; flip-angle = 150°; matrix size = 256×256; FOV = 240×240mm; slice thickness = 5.0mm; turbo factor = 5 slices = 32;). Functional MRI was performed using an echo-planner imaging (EPI)-based blood-oxygen-level-dependent (BOLD) sequence (TR = 2000ms, TE = 30ms, FA = 90°, matrix size = 64×64, FOV = 220×220mm, slices = 33, slice-thickness = 4.5mm, measurements = 180); these images were collected in the axial plane.

Cold Pressor Challenge—Following a 120 s baseline, the entire right foot was passively placed (placement duration <4 s, i.e., 2 scans) by two researchers into cold water (4°C) for a 120s foot immersion, followed by 120s recovery on foot removal. A subset of subjects assessed pain on a 0-10 scale (0, no pain; 10 maximum pain ever felt).

Data Analyses

Physiology—Respiratory and heart rates were calculated from the pressure and pulse oximeter signals respectively, and expressed as percentage change from the 120s baseline. Responses during the cold pressor challenge and recovery periods were compared with the mean baseline using repeated measures analysis of variance (RMANOVA), with Tukey-Fisher criteria for multiple comparisons (only variables with significant overall effects in the model were assessed for timepoint-by-timepoint differences). The SAS software procedure “proc mixed” was used to implement RMANOVA (SAS Enterprise Guide; SAS Institute Inc., Cary NC, USA).

MRI Pre-processing—High resolution T1-, PD-, and T2-weighted images were assessed in MRIcron (Rorden et al. 2007), to verify absence of gross brain pathology. Each scan was visually evaluated to verify the absence of cysts, infarcts, and other clinical pathologies. Functional scans were screened for obvious signal artifacts, such as gross inhomogeneities in signal intensity, large (>1%) step shifts in global signal intensities, and scans without “drop out” (where the whole scan intensity is close to zero, an occasional EPI-based imaging artifact).

Neural responses were evaluated with SPM8 software (SPM8; http://www.fil.ion.ucl.ac.uk/spm). The initial five volumes of each fMRI series were excluded to allow for signal saturation. The fMRI series were corrected for motion using the standard SPM "realign" procedure, and mean images calculated (images with motion >4mm were excluded). Any global fluctuations in the whole-brain global intensity, typically reflecting whole-brain blood volume changes, were removed using a detrending procedure. (Macey et al. 2004). The procedure subtracts any component matching the global signal (average of each scan over time) from each voxel, thus removing any variance correlated with whole brain blood volume changes. The unified segmentation approach was employed to determine normalization parameters, and used to spatially normalize the realigned images to the Montreal Neurological Institute reference space (Mazziotta et al. 1995). These normalized EPI images were then smoothed with a Gaussian filter (10mm), and neural responses to the challenge were examined via two procedures, whole-brain voxel-based analysis and structure-specific region of interest (ROI) sequential trend analysis.

A mean image was created for structural localization. High-resolution T1-weighted images for each subject were spatially normalized to the MNI space template. All subjects' normalized T1-weighted images were then averaged to create a group mean anatomical reference.

Functional MRI – Whole-brain Analysis—Pre-processed images were assessed with a fixed-effects paradigm, which utilized a finite impulse response (FIR) function with each time point being included as a variable in a linear model. Statistical parametric maps were derived for each volume, using contrasts applied to the model, and were compared to baseline by means of two-sample t-tests (uncorrected, $p<0.001$). Voxels which exhibited significant differences were color-coded and displayed over the mean background image.

Functional MRI – Structure-specific Analysis—Signal time courses within specific brain regions deemed relevant to the challenge by stimulation and other criteria were evaluated in individuals by analysis of manually-outlined ROIs, and included the left and right amygdala, insular cortices, and dorsal and ventral medulla, the hippocampi, caudate nuclei, thalamic and hypothalamic regions, dorsal and ventral pons, dorsal and ventral midbrain, dentate and fastigial nuclei of the cerebellum, and the anterior, mid, and posterior cingulate cortices (Harper et al. 2000; Kimmerly et al. 2005; Oppenheimer et al. 1992; Xu and Frazier 2002; Zamrini et al. 1990). Mean signal intensity across all voxels of a given ROI for each subject were calculated at 2s intervals throughout baseline, challenge and recovery periods. Signal changes observed during the challenge, relative to baseline, were assessed with RMANOVA ($p<0.05$) using SAS software. Group averages of time trends were plotted for each ROI.

To assess cold pressor response sequences, ROIs were classified into groups, based on significant signal change in timing or majority response. "Initial/early" group responses were large transient responses immediately after challenge onset, or occurred predominantly during the first half (0-60s). "Late" responses occurred during the second half (60-120s), and "prolonged" responses appeared for an extended period, including recovery.

Cross-correlations: Physiology and ROIs—To assess timing relationships between physiological and neural responses, both raw HR and respiratory rate values were cross-correlated with corresponding ROI signals for the 120s cold pressor challenge period. SPSS Statistics software (version 18, IBM, Chicago IL, USA) was used to generate a series of cross correlation functions (CCF), which were plotted such that the maximum amplitude, i.e. the time shift between neural and physiological responses, could be identified.

RESULTS

All subjects tolerated the entire foot immersion sequence. Pain ratings, recorded in a subset of six subjects, ranged from 3-10. Although MRI signals were analyzed from all 24 subjects, the physiological recordings of seven subjects were excluded for technical issues, including signal drop-out and movement artifacts; thus, the physiological findings were obtained from the 17 remaining subjects. A small number of isolated group differences emerged in amplitude and duration of neural responses between male and female subjects. Since these gender differences were modest and transient, only the whole-group data are presented.

Physiology

During the initial baseline period, mean heart and respiratory rates were 78.1 ± 0.2 bpm and 20.5 ± 0.1 breaths per minute, respectively. Following cold pressor administration, heart rate (HR) increased by 13.4 ± 2.7% ($p<0.0001$) during the initial 6s, and remained elevated for the stimulus duration, before declining below baseline (nadir = -9.0 ± 2.6%) throughout the recovery period (Fig. 1a). Respiratory rate responses were more variable, consisting of a transient increase within 5s of the challenge onset (21.9 ± 4.8%, $p<0.0001$), followed by a decline (12.9 ± 4.8%, $p=0.0075$), and a gradual return to baseline after approximately 75 s. A transient respiratory rate increase appeared at recovery onset (23.6 ± 4.8% after 4s, $p<0.0001$); however, baseline values re-established within only 9s (Fig. 1B).

Functional MRI – Whole brain Analysis

Whole-brain analyses of the functional fMRI signals identified significant changes in multiple brain regions throughout the cold pressor challenge, including areas of activation and decreased signals (Fig. 2). When the cold stimulus was administered (and after allowing 6s for hemodynamic delay (Liao et al. 2002), a brief activity increase emerged in the primary motor and sensory cortex for the lower body, prefrontal and parietal cortex, as well as declines in the anterior, mid, and posterior cingulate cortex, lateral and anterior thalamus, hippocampus, and lateral temporal cortex and the dorsal cortex and vermis of the cerebellum. Sustained changes also appeared throughout the challenge period, including signal increases in the medial parietal somatosensory cortex, and declines in the caudate nucleus and posterior cingulate cortex; these effects were bilateral, although activation in the somatosensory cortex was more prominent on the left side.

Functional MRI – VOI Analysis

Timing of the cold pressor responses varied between different ROIs, and signal changes were classified as initial/early, prolonged, and late. Furthermore, the timing sequences differed between left and right sides in some structures.

Early Responses—Initial signal patterns to the cold challenge were transient in nature in some ROIs (Fig. 3 and 4). Significantly increased signals appeared in the medulla within the first 5s of the challenge, with the largest peak in the ventral medulla (0.93% increase) at 16s; baseline signals resumed after 25s (Fig. 3a). In addition, immediately following cold onset, rapid signal declines appeared in the hypothalamus, thalamus, caudate nucleus, hippocampus, fastigial nucleus, anterior and mid-cingulate cortex. Signals returned to baseline after various intervals (range, 5-75s), and responses were bilateral, with the exception of the right thalamus (Fig. 4a).

Late Responses—Despite initial transient signal declines, the anterior and mid-cingulate regions increased activity from approximately 50-60s, throughout the remaining half of cold pressor application. Conversely, the thalamus, hippocampus, fastigial and caudate nuclei showed similar or more-modest, yet statistically significant, declines in signal activity (Fig. 4a, b, c and 3c respectively). In addition, dorsal and ventral pontine signals fell below baseline toward the end of the challenge. After cold stimulus removal, dorsal pontine signal changes recovered within 10-15s; however, ventral pontine signals continued to rise, and remained elevated during recovery (Fig. 4d).

Prolonged Responses—Left and right posterior cingulate activity declined for the entire cold pressor challenge, with a further decrease observed at challenge offset before returning to baseline (Fig. 5a). Signals in both anterior and posterior insular cortices gradually rose throughout the challenge, and remained approximately 0.5% above baseline for the duration of the recovery period, with the exception of a brief return to baseline immediately following challenge offset (Fig. 5b and c). A similar response pattern also developed in the amygdalae, where augmented signals appeared by 20s into the challenge and persisted throughout the recovery period bilaterally (Fig. 5d).

Response Laterality—Some ROIs responded differently between sides, such as the hypothalamus and deep cerebellar nuclei. Although cold onset was associated with decreased signals in both the left and right hypothalamus, responses were larger (0.6% vs. 0.3%) and longer (approximately 75s vs. 40s) on the left side (Fig. 3b). Similar pattern differences between sides emerged in the declining signals of the fastigial nuclei during the last half of the challenge (Fig. 4c). In the left dentate nucleus, signals were reduced throughout the cold application, returning to baseline within seconds of foot removal from cold water. In contrast, right dentate nucleus responses were inconsistent during the challenge (slight increase initially, followed by a decline below baseline) before remaining elevated for the entire recovery (Fig. 5e). Responses in the left and right dentate nuclei closely reflected the dorsal and ventral pons, respectively (Fig. 4d).

Cross-correlations: Physiology and ROIs

During the cold application, HR accelerated as the ventral medulla signal increased (cross-correlation function, CCF = 0.57), with a time delay of 2s (Fig. 6a). In addition, a strong negative correlation (CCF = -0.62), with a lag of 8 s appeared between HR and signals in the left insular cortex. A similar, although weaker (CCF = -0.4), relationship emerged with the right insula. Lateralized pattern differences were comparable between the posterior regions

and anterior insular cortices (Fig. 6b,c). No significant correlations appeared between respiratory rate and the ROIs.

DISCUSSION

Cold application to the foot elicited expected signal changes in primary sensory areas, as well as in autonomic regulatory areas from the forebrain to the medulla, and the cerebellum. Physiological responses differed from those found earlier in similarly-aged adolescents with trigeminal pathway cold-forehead application (Kim et al. 2002). Instead of declining heart and respiratory rates from the trigeminally-mediated dive reflex, HR increased significantly to cold foot stimulation, and remained elevated for the entire challenge, before slowing to 10% below baseline during recovery. In contrast, breathing rates decreased below baseline within 15s of an initial rise, and gradually recovered prior to cold offset. FMRI signal patterns associated with the heart and respiratory rate changes were often lateralized, and showed early and late activation of sensory and autonomic regulatory areas and their modulatory regions (Figures 1-6). The modulatory regions include the cerebellum and cortical regions, which the current findings confirm play key roles in control of responses to blood pressure elevation or deviations in those responses in pathological conditions. The asymmetric insular patterns likely reflect differentiation of sympathetic and parasympathetic roles in timing, while the late cerebellar responses in the recovery period may underlie impaired recovery in other pathologic adult cold pressor challenges, such as the delayed recovery of heart rate in obstructive sleep apnea (Harper et al., 2003).

Right foot cold application initially activated the medial parietal somatosensory cortex bilaterally (sensory area for the lower body), but more-prominently on the left side. Large signal increases also appeared in the medulla, primarily the ventral medulla, very early, which returned to baseline after 25s. During the second half of the challenge (60-120s), modest increases appeared in the anterior and midcingulate cortices; decreased signals also emerged during this period in the caudate nuclei, hippocampi, dentate and fastigial nuclei of the cerebellum, thalami and pons. Signal increases in the insular cortices and amygdalae, and declines in the posterior cingulate remained sustained for the entire cold stimulation period. Central responses to peripheral cold stimulation differed substantially from our earlier forehead trigeminal stimulation studies, which elicited increased BOLD signals in the dorsal pons, as well as the caudate, dentate and fastigial nuclei, and mid/posterior cingulate cortices in similarly-aged adolescents and in adults (Harper et al. 2003; Macey et al. 2005). The specificity of central and physiological responses to the nature of stimulation (peripheral vs. trigeminal) has been noted by others (Durel et al. 1993). Forehead application of cold in the earlier studies also elicited signals that were distorted by close proximity of brain tissue with water condensate around a cold sac of deuterium used as a stimulus. Peripheral foot application of cold has no such problems.

Early activation in the medulla was expected, given the cold pressor challenge, which rapidly initiates a baroreflex response, integrating afferent activity and stimulating ventral medullary areas forming the final common path from sympathetic regulatory areas to the spinal cord. Neural responses are reflected in the physiological recordings; although heart rate remained elevated throughout the entire challenge, that rate dropped considerably (by

half) after approximately 25s, followed closely by medullary signals declining to baseline. The parallel interaction of heart rate and medullary responses likely reflects increased blood pressure accompanying the cold pressor challenge. Continuous blood pressure measurements were not feasible for this study, since no viable non-invasive MRI-compatible technology existed at the time of recording; however, non-MRI studies of comparable adolescent controls report significantly increased mean, diastolic, and systolic blood pressures within the first minute of similar cold pressor application (Nageswari et al. 2007). Signal declines in the cerebellar fastigial nuclei during the second minute likely reflect central responses to increased blood pressure; we earlier showed in a rodent model that the fastigial nucleus was similarly deactivated following an induced hypertensive event (Rector et al. 2006). The deep cerebellar nuclei are significant structures for autonomic modulation of blood pressure and breathing (Xu and Frazier 2002). Although a cerebellar response would be expected during vestibular pressor challenges (Miura and Reis 1969), the cerebellum also responds to cold-initiated elevated blood pressure.

A close interaction exists between breathing control and momentary blood pressure changes, with transient hypotension inducing increased ventilation (Harper et al. 1999), and transient hypertension suppressing upper airway and diaphragmatic action (Marks and Harper 1987). The most marked changes in breathing patterns were the transient increases in frequency at both onset and offset of the cold pressor application. Concurrent declines in BOLD signals also occurred in some ROIs; the largest effects appeared bilaterally in the caudate nucleus and hippocampus, although the thalamus also demonstrated a dramatic signal decline at recovery onset. Foot placement to cold water was passive to minimize central voluntary contributions to neural activity. Despite these efforts, a portion of the transient changes observed at challenge onset and offset may have resulted from sensory stimulation and movement related to placing the foot into water. MR images were examined closely, and any displaying noticeable movement artifacts were excluded from analyses; therefore, it is likely that these transient changes reflect a sensory component or transient autonomic response to the sudden temperature change.

Modest signal increases appeared in the anterior and mid-cingulate cortex during the challenge in addition to transient on and off responses. The cingulate cortex has extensive projections to multiple limbic structures, and participates in emotion formation and processing, executive function, as well as intricate control of upper airway musculature and blood pressure (Corfield et al. 1995; Gianaros et al. 2005; Lane et al. 1998). Separate functions of the cingulate cortex are mediated by specific sub-regions, as demonstrated by the different cold pressor responses between anterior and posterior cingulate. The dorsal anterior cingulate controls some aspects of sympathetic outflow and autonomic reactivity (Matthews et al. 2004). A role for pain perception has also been noted for the anterior cingulate (Fulbright et al. 2001).

Activity in the anterior cingulate cortex appears to be influenced by the medial prefrontal and anterior insular cortices, relationships that occur at rest and during an autonomic challenge (Peckerman et al. 1994; Peltz et al. 2011; Ryan et al. 2011). Throughout the cold pressor challenge, signals consistently increased in the left and right insular cortices, in both anterior and posterior regions. Both insulae contribute to autonomic regulation, with the left

and right sides showing a bias towards modulating parasympathetic and sympathetic activity respectively (Oppenheimer et al. 1992). This relationship is reflected in the rapid increase of signals in the right anterior insula, followed approximately 20s later on the left side. Cross-correlations further demonstrate functional lateralization of the insula; activation of the left insula accompanied a gradual decline in HR within 8s. In addition to autonomic regulatory roles, the anterior insula serves a major role for pain perception (Henderson et al. 2007). The posterior insula, however, receives information from the ventromedial nucleus of the thalamus relating to touch, pain and thermal stimulation, and is more closely associated with sensing and classifying noxious and somatosensory stimuli (Craig 2011; Peltz et al. 2011). Bilateral signal increases in the posterior insula emerged immediately following cold pressor onset, and plateaued after approximately 30s. Signals remained elevated throughout the challenge, long after any novel tactile stimulation had subsided; hence, these changes likely reflect the thermal or nociceptive response. Bilateral responses in the thalamus likely reflect projections of arousal arising from periaqueductal gray and reticular activating structures mediating cold and wetness afferents from unilateral spinal pathways.

The normal temporal sequencing of central processes during autonomic challenges can provide useful insights into failed autonomic regulatory mechanisms in certain pathological conditions. Pediatric disorders with autonomic dysfunction frequently distort timing and amplitude of neural activity mediating autonomic processing, as demonstrated by compromised regulation of cardiovascular and central patterns found in several pediatric syndromes, including obstructive sleep apnea, congenital central hypoventilation, Dravet, Prader-Willi, Rett, and Sickle Cell Anemia (Axelrod et al. 2006; Delogu et al. 2011; Sangkatumvong et al. 2011). To determine the central processes underlying exaggerated or diminished sympathetic or parasympathetic tone in these conditions, normal responses of autonomic regulatory areas to common challenges must be assessed. These normative data elucidate how the brain mounts normal physiological responses, and the present data can be used as references against which disease processes with autonomic involvement can be compared.

Limitations

Cold pressor application could potentially influence global cerebral circulation via sympathetic influences on the vasculature. To ensure a focus on regional responses to the challenge, we removed all global effects in the BOLD signal during image pre-processing (Macey et al. 2004). A difficulty in discriminating differential contributions from other sensory processes accompanying the challenge is also a limitation. Central representation for cold, pain, and touch cannot readily be separated; the cingulate and insular cortices respond to all three stimuli (Craig 2011), although the topography for each are still being mapped. Central voluntary movement representation was minimized by passively moving the foot into cold water. Nociceptive afferents may have been stimulated; however the water temperature (4°C), was warmer than the 0-1°C typically used in pain studies (Neziri et al. 2011) and reports of significant pain were not an issue. Even with these limitations, the foot cold pressor was considered the most appropriate stimulus for this investigation. While other autonomic tasks, such as handgrip, could have been useful for autonomic assessment (Wong

et al. 2007), the handgrip challenge involves sustained voluntary motor effort, whereas the cold pressor avoids that component by inducing what is primarily a reflexive response.

Despite continuing the physiological recordings and MRI scans for 120s following cold pressor application, the recovery time was insufficient for all signals to return to baseline levels. Signals in the insular cortices and amygdalae remained elevated for almost the entirety of the recovery period, with only a mild declining trend in the posterior insula. Changes in some responses appeared during the recovery period; HR fell significantly below baseline, and remained low for the remaining scans. Similar signal declines appeared in the left thalamus, while the right dentate nucleus, ventral pons, and right hippocampus all exhibited the opposite pattern, i.e. an increase in signals post-stimulus. We could not resolve the time required for these responses to return to baseline from these data.

There were 24 subjects included in the fMRI analyses and adequate physiological data were obtained for 17 subjects. When fMRI time trends were generated for those 17 subjects alone (not shown), the resulting responses were nearly identical to all 24 individuals; therefore, data from the larger subject group (n=24) were reported to ensure higher statistical power. We studied a rather broad range of ages (11-18 years), during which dramatic brain growth and maturation occurs (Gogtay et al. 2004; Kumar et al. 2012). The potential for these structures to respond differently over this developmental period should be recognized; however dramatic effects of age are unlikely, since the majority of subjects were close to the median age of 15 (interquartile range = 3).

CONCLUSIONS

Both transient and sustained responses emerged in multiple brain sites to a foot cold pressor challenge in these healthy adolescents. The signal changes in the primary somatosensory cortex were accompanied by responses in multiple brain areas which influence sympathetic and parasympathetic regulation, with onset and offset transients appearing in some limbic areas. The recruitment of brain structures to mediate this autonomic challenge followed a systematic and lateralized pattern, beginning with the somatosensory cortex and medulla, followed by the caudate nuclei, cingulate and insular cortices, amygdalae, cerebellum, thalamus and pons. This amplitude and timing sequence will likely differ in a pathological condition, and these normative findings will assist understanding of mechanisms underlying deficient autonomic responses.

Acknowledgments

The authors thank Rebecca Harper for assistance with data collection.

Grant support: This research was supported by R01 HD22695 (RMH), R01 HL113251 (RK), R01 NR013693 (PMM), and NHMRC CJ Martin Fellowship 606770 (HLR).

REFERENCES

Axelrod FB, Chelimsky GG, Weese-Mayer DE. Pediatric autonomic disorders. Pediatrics. 2006; 118(1):309–321. [PubMed: 16818580]

Corfield DR, Fink GR, Ramsay SC, Murphy K, Harty HR, Watson JD, Adams L, Frackowiak RS, Guz A. Evidence for limbic system activation during CO2-stimulated breathing in man. J Physiol. 1995; 488(Pt 1):77–84. [PubMed: 8568667]

Craig AD. Significance of the insula for the evolution of human awareness of feelings from the body. Ann N Y Acad Sci. 2011; 1225:72–82. [PubMed: 21534994]

Delogu AB, Spinelli A, Battaglia D, Dravet C, De Nisco A, Saracino A, Romagnoli C, Lanza GA, Crea F. Electrical and autonomic cardiac function in patients with Dravet syndrome. Epilepsia 52 Suppl. 2011; 2:55–58.

Durel LA, Kus LA, Anderson NB, McNeilly M, Llabre MM, Spitzer S, Saab PG, Efland J, Williams R, Schneiderman N. Patterns and stability of cardiovascular responses to variations of the cold pressor test. Psychophysiology. 1993; 30(1):39–46. [PubMed: 8416061]

Fulbright RK, Troche CJ, Skudlarski P, Gore JC, Wexler BE. Functional MR imaging of regional brain activation associated with the affective experience of pain. Am J Roentgenol. 2001; 177(5): 1205–1210. [PubMed: 11641204]

Gianaros PJ, Derbyshire SW, May JC, Siegle GJ, Gamalo MA, Jennings JR. Anterior cingulate activity correlates with blood pressure during stress. Psychophysiology. 2005; 42(6):627–635. [PubMed: 16364058]

Gogtay N, Giedd JN, Lusk L, Hayashi KM, Greenstein D, Vaituzis AC, Nugent TF 3rd, Herman DH, Clasen LS, Toga AW, Rapoport JL, Thompson PM. Dynamic mapping of human cortical development during childhood through early adulthood. Proc Natl Acad Sci U S A. 2004; 101(21): 8174–8179. [PubMed: 15148381]

Harper RM, Bandler R, Spriggs D, Alger JR. Lateralized and widespread brain activation during transient blood pressure elevation revealed by magnetic resonance imaging. J Comp Neurol. 2000; 417(2):195–204. [PubMed: 10660897]

Harper RM, Macey PM, Henderson LA, Woo MA, Macey KE, Frysinger RC, Alger JR, Nguyen KP, Yan-Go FL. fMRI responses to cold pressor challenges in control and obstructive sleep apnea subjects. J App Physiol. 2003; 94(4):1583–1595.

Harper RM, Richard CA, Rector DM. Physiological and ventral medullary surface activity during hypovolemia. Neuroscience. 1999; 94(2):579–586. [PubMed: 10579218]

Henderson LA, Gandevia SC, Macefield VG. Somatotopic organization of the processing of muscle and cutaneous pain in the left and right insula cortex: a single-trial fMRI study. Pain. 2007; 128(1-2):20–30. [PubMed: 17011704]

Kim AH, Macey PM, Woo MA, Yu PL, Keens TG, Gozal D, Harper RM. Cardiac responses to pressor challenges in congenital central hypoventilation syndrome. Somnologie. 2002; 6:109–115.

Kimmerly DS, O'Leary DD, Menon RS, Gati JS, Shoemaker JK. Cortical regions associated with autonomic cardiovascular regulation during lower body negative pressure in humans. J Physiol. 2005; 569(Pt 1):331–345. [PubMed: 16150800]

Kumar R, Nguyen HD, Macey PM, Woo MA, Harper RM. Regional brain axial and radial diffusivity changes during development. J Neurosci Res. 2012; 90(2):346–355. [PubMed: 21938736]

Lane RD, Reiman EM, Axelrod B, Yun LS, Holmes A, Schwartz GE. Neural correlates of levels of emotional awareness. Evidence of an interaction between emotion and attention in the anterior cingulate cortex. J Cogn Neurosci. 1998; 10(4):525–535. [PubMed: 9712681]

Liao CH, Worsley KJ, Poline JB, Aston JA, Duncan GH, Evans AC. Estimating the delay of the fMRI response. Neuroimage. 2002; 16(3 Pt 1):593–606. [PubMed: 12169246]

Lovallo W. The cold pressor test and autonomic function: a review and integration. Psychophysiology. 1975; 12(3):268–282. [PubMed: 1153632]

Macey PM, Macey KE, Kumar R, Harper RM. A method for removal of global effects from fMRI time series. Neuroimage. 2004; 22(1):360–366. [PubMed: 15110027]

Macey PM, Macey KE, Woo MA, Keens TG, Harper RM. Aberrant neural responses to cold pressor challenges in congenital central hypoventilation syndrome. Pediatr Res. 2005; 57(4):500–509. [PubMed: 15718375]

Marks JD, Harper RM. Differential inhibition of the diaphragm and posterior cricoarytenoid muscles induced by transient hypertension across sleep states in intact cats. Exp Neurol. 1987; 95(3):730–742. [PubMed: 3817089]

Matthews SC, Paulus MP, Simmons AN, Nelesen RA, Dimsdale JE. Functional subdivisions within anterior cingulate cortex and their relationship to autonomic nervous system function. Neuroimage. 2004; 22(3):1151–1156. [PubMed: 15219587]

Mazziotta JC, Toga AW, Evans A, Fox P, Lancaster J. A probabilistic atlas of the human brain: theory and rationale for its development. The International Consortium for Brain Mapping (ICBM). Neuroimage. 1995; 2(2):89–101. [PubMed: 9343592]

Miura M, Reis DJ. Cerebellum: a pressor response elicited from the fastigial nucleus and its efferent pathway in brainstem. Brain Res. 1969; 13(3):595–599. [PubMed: 5772438]

Nageswari KS, Sharma R, Kohli DR. Assessment of respiratory and sympathetic cardiovascular parameters in obese school children. Indian J Physiol Pharmacol. 2007; 51(3):235–243. [PubMed: 18341219]

Neziri AY, Scaramozzino P, Andersen OK, Dickenson AH, Arendt-Nielsen L, Curatolo M. Reference values of mechanical and thermal pain tests in a pain-free population. Eur J Pain. 2011; 15(4):376–383. [PubMed: 20932788]

Oppenheimer SM, Gelb A, Girvin JP, Hachinski VC. Cardiovascular effects of human insular cortex stimulation. Neurology. 1992; 42(9):1727–1732. [PubMed: 1513461]

Peckerman A, Hurwitz BE, Saab PG, Llabre MM, McCabe PM, Schneiderman N. Stimulus dimensions of the cold pressor test and the associated patterns of cardiovascular response. Psychophysiology. 1994; 31(3):282–290. [PubMed: 8008792]

Peltz E, Seifert F, DeCol R, Dorfler A, Schwab S, Maihofner C. Functional connectivity of the human insular cortex during noxious and innocuous thermal stimulation. Neuroimage. 2011; 54(2):1324–1335. [PubMed: 20851770]

Rector DM, Richard CA, Harper RM. Cerebellar fastigial nuclei activity during blood pressure challenges. J App Physiol. 2006; 101(2):549–555.

Rorden C, Karnath HO, Bonilha L. Improving lesion-symptom mapping. J Cogn Neurosci. 2007; 19(7):1081–1088. [PubMed: 17583985]

Ryan JP, Sheu LK, Gianaros PJ. Resting state functional connectivity within the cingulate cortex jointly predicts agreeableness and stressor-evoked cardiovascular reactivity. Neuroimage. 2011; 55(1):363–370. [PubMed: 21130172]

Sangkatumvong S, Khoo MC, Kato R, Detterich JA, Bush A, Keens TG, Meiselman HJ, Wood JC, Coates TD. Peripheral vasoconstriction and abnormal parasympathetic response to sighs and transient hypoxia in sickle cell disease. Am J Respir Crit Care Med. 2011; 184(4):474–481. [PubMed: 21616995]

Wong SW, Kimmerly DS, Masse N, Menon RS, Cechetto DF, Shoemaker JK. Sex differences in forebrain and cardiovagal responses at the onset of isometric handgrip exercise: a retrospective fMRI study. J App Physiol. 2007; 103(4):1402–1411.

Xu F, Frazier DT. Role of the cerebellar deep nuclei in respiratory modulation. Cerebellum. 2002; 1(1):35–40. [PubMed: 12879972]

Zamrini EY, Meador KJ, Loring DW, Nichols FT, Lee GP, Figueroa RE, Thompson WO. Unilateral cerebral inactivation produces differential left/right heart rate responses. Neurology. 1990; 40(9): 1408–1411. [PubMed: 2392227]

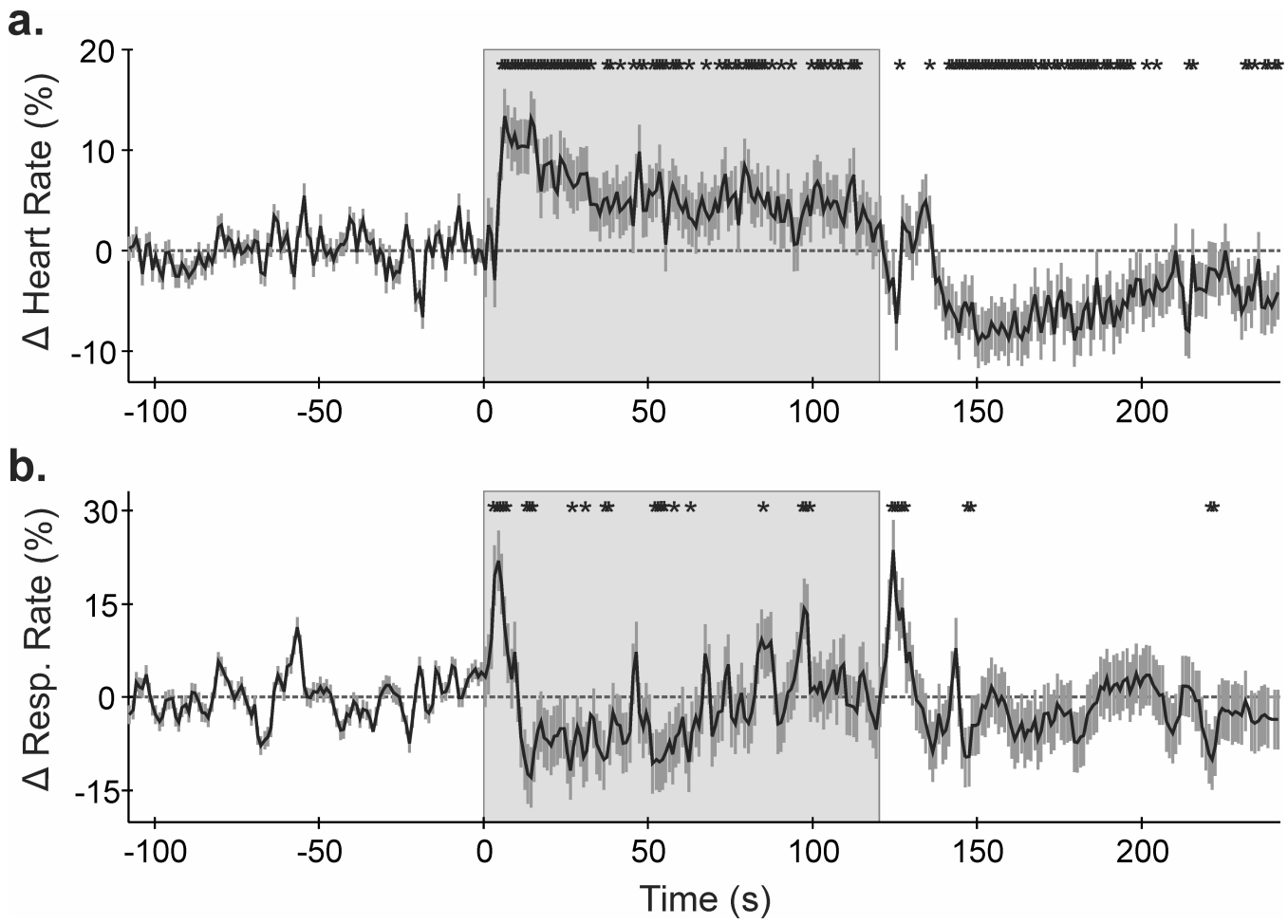

Figure 1.

Mean ± SEM (a) heart rate and (b) respiratory rate over time (% from baseline). *p<0.05, RMANOVA; shaded area = cold stimulation period.

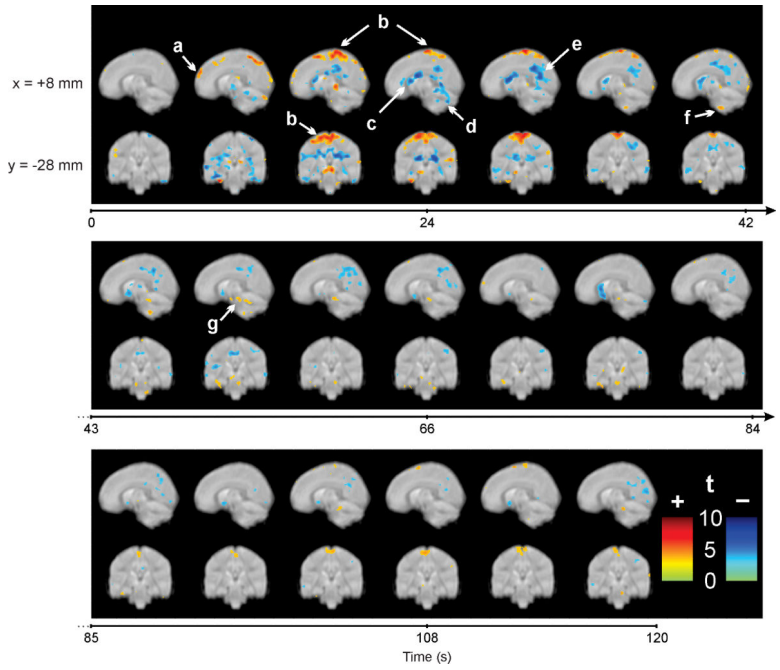

Figure 2.

Whole-brain voxel-based analysis during the 120s cold pressor challenge, showing examples of increased (+, warm colors) and decreased (-, cool colors) signal intensities, relative to the pre-stimulus baseline; (a) prefrontal cortex, (b) somatosensory cortex, (c) left caudate nucleus, (d) dorsal cerebellum, (e) left posterior cingulate, (f) ventral cerebellum, (g) substantia nigra. Color scales indicate statistical significance (t statistic). Slice locations are in MNI space; sagittal view, x= +8mm; coronal view, y= -28mm. Time 0 represents cold pressor initiation.

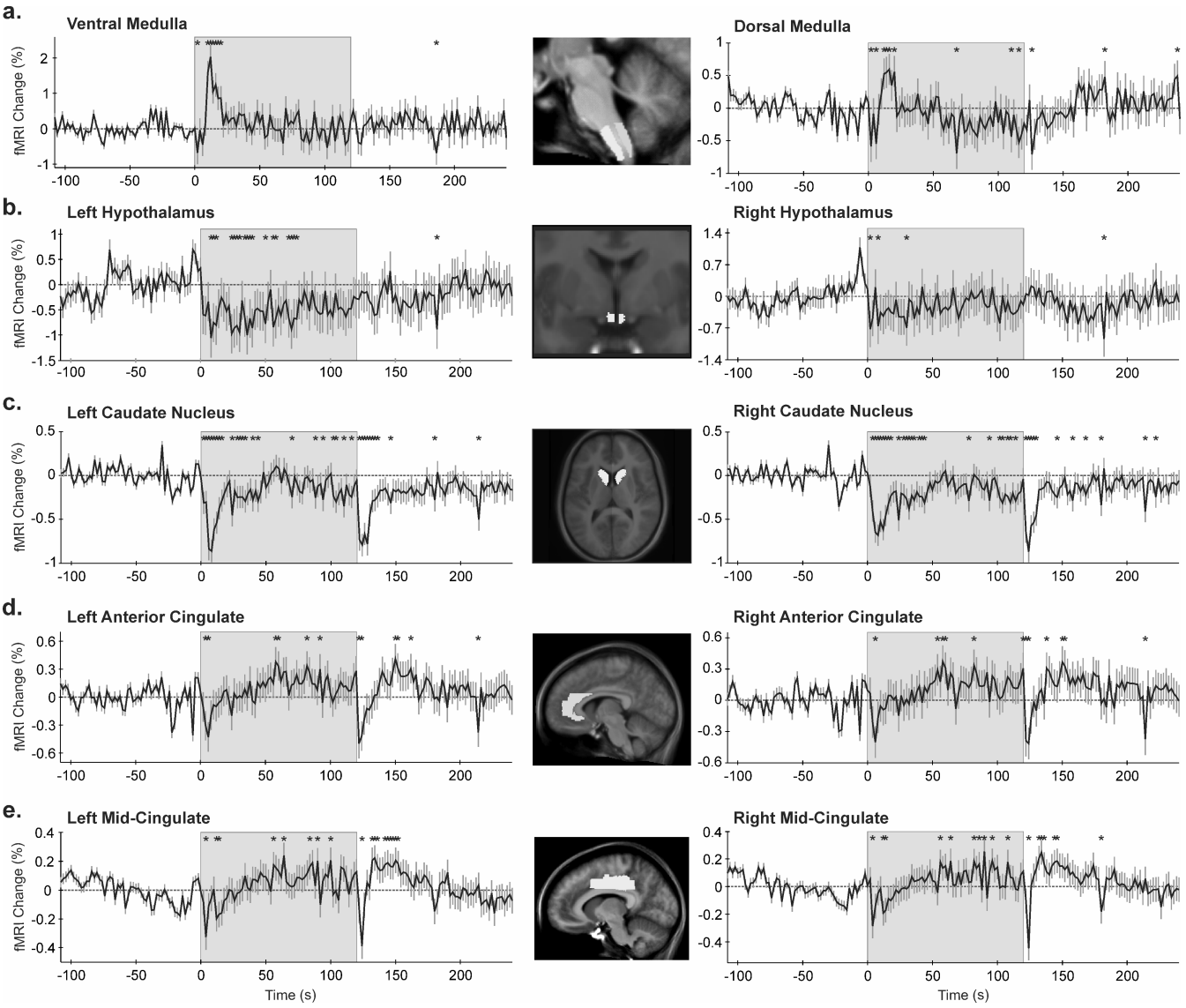

Figure 3.

Regions of interest (ROIs, highlighted in the inset) and corresponding time trends (% from baseline); (a) medulla, (b) hypothalamus, (c) caudate nucleus, (d,e) anterior and middle cingulate cortices. *p<0.05, RMANOVA; shaded area = cold stimulation period.

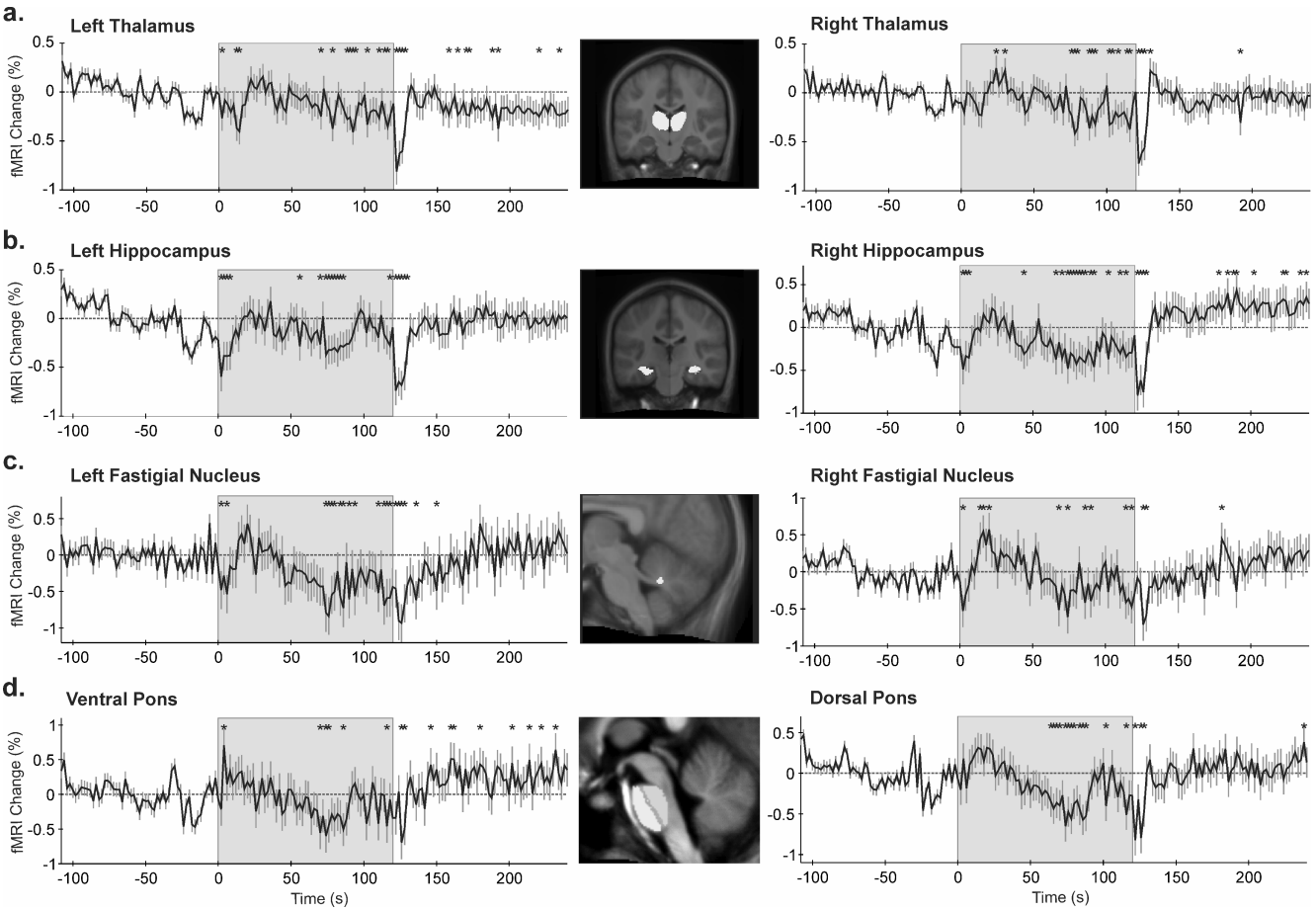

Figure 4.

Regions of interest (ROIs, highlighted in the inset) and corresponding time trends (% from baseline); (a) thalamus, (b) hippocampus, (c) fastigial nucleus, (d) pons. *p<0.05, RMANOVA; shaded area = cold stimulation period.

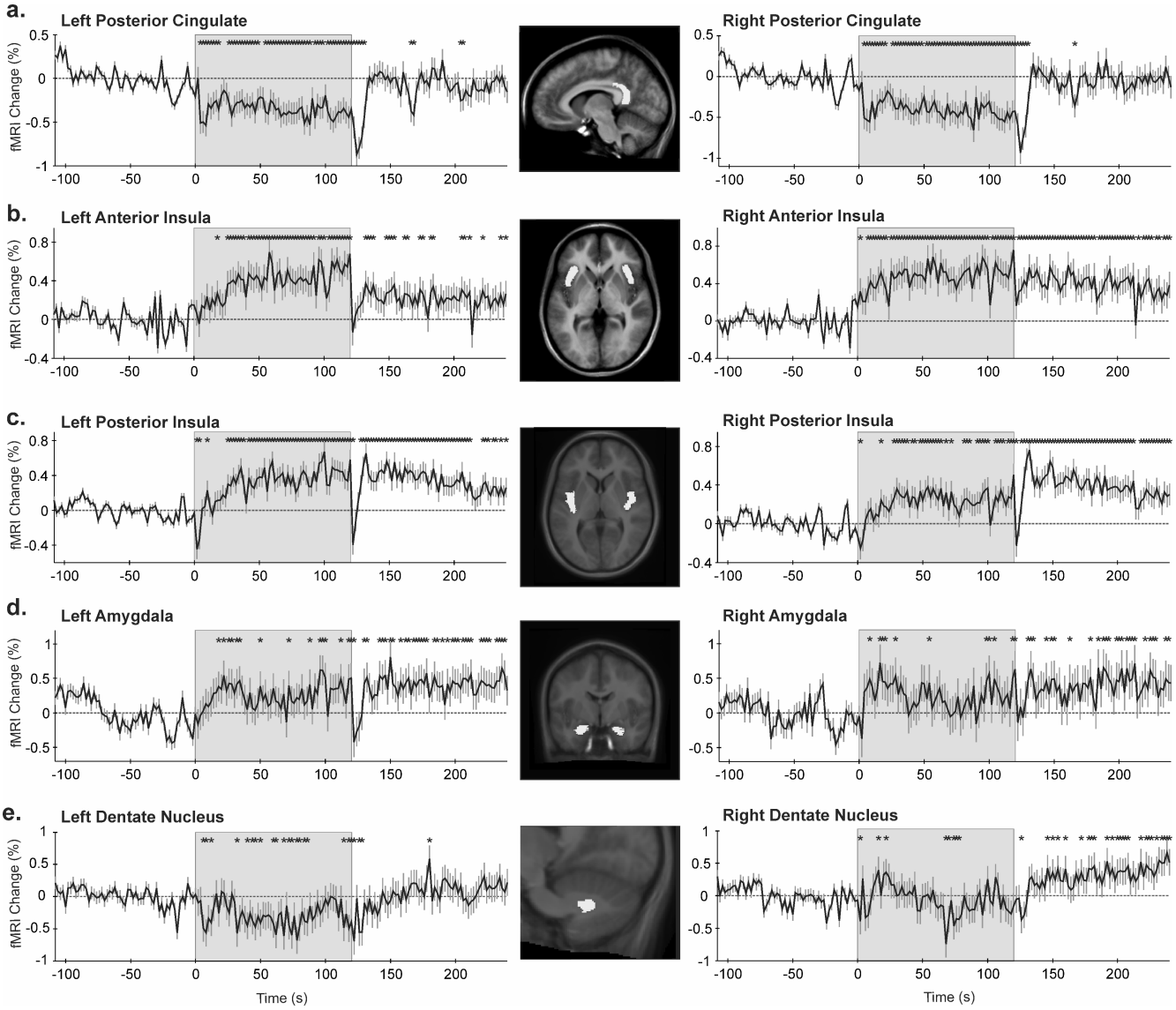

Figure 5.

Regions of interest (ROIs, highlighted in the inset) and corresponding time trends (% from baseline); (a) posterior cingulate cortex, (b,c) anterior (including sub-genu) and posterior insular cortices, (d) amygdala, (e) dentate nucleus. *p<0.05, RMANOVA; shaded area = cold stimulation period.

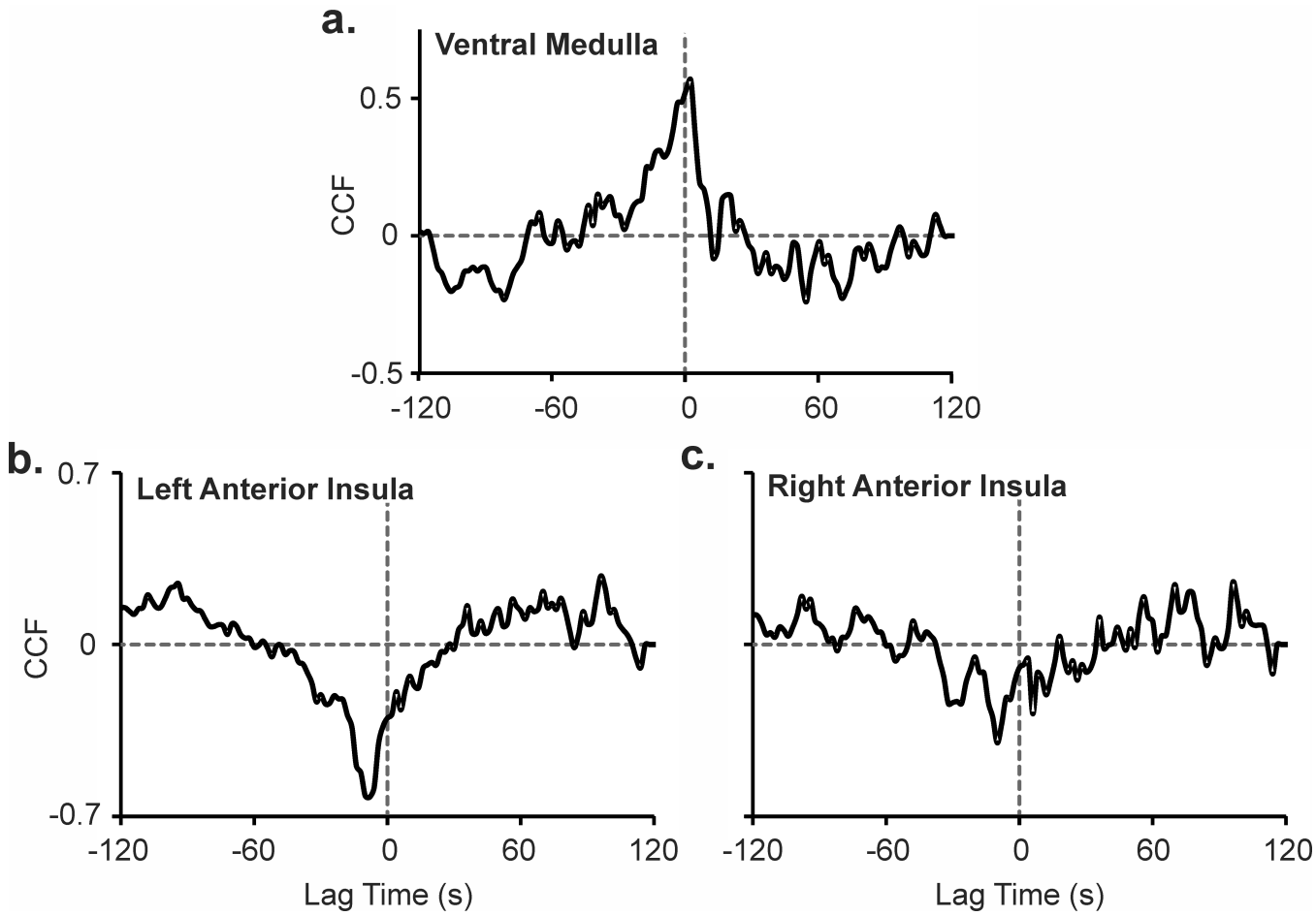

Figure 6.

Heart rate response during a cold pressor challenge, cross-correlated with signals from (a) ventral medulla, and (b) left and (c) right anterior insular cortices; cross-correlation function (CCF) at various time lags.